doi: 10.18323/2782-4039-2024-2-68-8

Acoustic properties of 15-5 PH maraging steel after energy deposition

Olga V. Muravieva[1,2,3], Doctor of Sciences (Engineering), Professor,
professor of Chair "Instruments and Methods of Measurements, Testing, Diagnostics"
Vitaly V. Muraviev[1,2,4], Doctor of Sciences (Engineering), Professor,
professor of Chair "Instruments and Methods of Measurements, Testing, Diagnostics"
Lyudmila V. Volkova[1,5], PhD (Engineering), Associate Professor,
assistant professor of Chair "Instruments and Methods of Measurements, Testing, Diagnostics"
Aleksey L. Vladykin*[1,6], postgraduate student
Konstantin Yu. Belosludtsev[1], graduate student
[1]*Kalashnikov Izhevsk State Technical University, Izhevsk (Russia)*
[2]*Udmurt Federal Research Center of the Ural branch of the RAS, Izhevsk (Russia)*

***E-mail:** pmkk@istu.ru,
vladykin-ndt@mail.ru

[3]ORCID: https://orcid.org/0000-0003-3442-8163
[4]ORCID: https://orcid.org/0000-0001-8590-1382
[5]ORCID: https://orcid.org/0000-0001-5128-6465
[6]ORCID: https://orcid.org/0009-0006-1813-2011

Received 05.07.2023 *Accepted 28.11.2023*

Abstract: The study of the acoustic properties of maraging steels operated under various energy force and temperature actions is a critical task, since it is the method of acoustic structuroscopy that provides the most reliable connection with the structure, stress-strain state and mechanical properties of steels. The paper is devoted to research of the acoustic properties of the 15-5 PH maraging steel samples under various types of heat treatment under the conditions of mechanical tensile and cyclic loads. Samples of the 15-5 PH maraging steel were studied in three structural states: solid solution annealing and subsequent aging at 470 and 565 °C; during tensile tests; during cyclic tension-compression loading. The research used a unique scientific installation "Information-measuring complex for investigation of acoustic properties of materials and products". It implements the acoustic mirror-shadow multiple reflections method using electromagnetic-acoustic and piezoelectric transducers based on polyvinylidene fluoride film to excite and receive waves and allows determining the velocity of wave propagation with an error of no more than 2 m/s. The acoustic (wave velocity, elastic moduli, electromagnetic-acoustical (EMA) transformation coefficients, acoustic anisotropy coefficients, acoustoelastic coupling coefficients) and electromagnetic (coercive force and electrical conductivity) characteristics of the samples were examined. The samples were studied in the initial state (before loading); stepwise in the process of tensile loads and subsequent unloading; after tensile tests; during cyclic tension-compression loading. It was revealed that the following acoustic parameters of 15-5 PH steel samples are the greatest structural sensitivity to mechanical tensile load and cyclic loading: transverse wave velocity, Poisson's ratio, double EMA-transformation coefficient, and acoustic anisotropy coefficient.

Keywords: 15-5 PH maraging steel; acoustic properties; heat treatment; mechanical tensile load; cyclic loading.

Acknowledgements: The study was supported by the grant of the Russian Science Foundation (project No. 22-19-00252, https://rscf.ru/project/22-19-00252/) using the Unique Scientific Installation "Information-measuring complex for investigation of acoustic properties of materials and products" (registration number 586308).

The paper was written on the reports of the participants of the XI International School of Physical Materials Science (SPM-2023), Togliatti, September 11–15, 2023.

For citation: Muravieva O.V., Muraviev V.V., Volkova L.V., Vladykin A.L., Belosludtsev K.Yu. Acoustic properties of 15-5 PH maraging steel after energy deposition. *Frontier Materials & Technologies*, 2024, no. 2, pp. 87–100. DOI: 10.18323/2782-4039-2024-2-68-8.

INTRODUCTION

Maraging steels are widely used in many industries due to their high strength and toughness without loss of ductility and increased heat resistance with a low cold brittleness threshold. High mechanical properties of these steels are achieved by the use of alloying elements, an important component of which is nickel, as well as chromium, copper, cobalt, titanium, manganese, silicon, etc. Heat treatment of maraging steels consists of solid solution annealing and subsequent aging in the temperature range of 400...550 °C, which makes the greatest contribution to strengthening [1]. Maraging steels are used for heavy-duty parts operated under conditions of cyclic force and temperature exposure, at extremely high and low temperatures.

The KhM-12 steel discussed in this paper, also known as 15-5 PH or UNS S15500, contains chromium, nickel and copper as alloying elements. Its unique structure ensures increased strength and corrosion resistance, improved

toughness and a quenching temperature lower than its predecessor, 17-4 PH steel, does [2].

In many foreign publications dealing with 15-5 PH maraging steel, the influence of heat treatment modes on the microstructure and mechanical properties of this steel is studied using destructive methods on special samples cut from industrial products [3–7]. In particular, in [3], using electron microscopy, it was shown that the microstructure of martensitic stainless steel undergoes a complex evolution during long-term aging. This evolution includes the possible development of a minor austenitic phase, copper-rich precipitates, and the precipitation of chromium and silicon from the solid solution. Precipitates several nm in size coherently nucleate during aging at the interfaces with the matrix. With longer aging, clusters are uniformly formed in the matrix.

It was shown in [4] that the tensile strength of a martensitic steel weld first increases with the growth of aging temperature after welding, which is associated with the size and distribution of the copper-rich phase, and then decreases with the growth of aging temperature after welding, probably due to an increase in amount of residual austenite.

The results of [5] showed that the tensile strength of stainless steel first decreased with increasing aging temperature from 440 to 540 °C, and then increased with increasing aging temperature from 540 to 610 °C. The authors believe that hardening mechanisms caused by the dislocation density and deposition of a second phase enriched in copper precipitates at various aging temperatures are the predominant strengthening mechanisms.

In [6], cyclic bending tests were carried out on samples made of martensitic stainless steel to determine fatigue strength. The study showed that the influence of the compressive sublayer on fatigue strength is much more important than the influence of surface roughness or microstructure. In [7], electron microscopic studies identified that the strengthening of grain boundaries by dislocations and the resulting copper precipitates in 15-5 PH martensitic stainless steel is the main factor determining the increase in the tensile strength and yield of tempered martensite.

Many recent studies deal with the analysis of the microstructure and mechanical properties of maraging steels produced using additive technologies [8–10], including during cyclic tests [11]. For example, the work [8] notes that the hardness of the metal produced by direct laser sintering varies along the upper and lower parts of the finished samples and the hardness of the upper part of the samples is higher due to the finer grain size. However, aging of the alloy promotes further increase in its hardness and strength. The work [9] shows that the amount of residual austenite is significantly reduced after heat treatment, and the remaining minor residual austenite is completely converted to martensite during mechanical tension in samples produced by selective laser melting. Standard aging conditions increase the yield stress, hardness and corrosion resistance of steel through the formation of fine spherical copper-rich deposits, but make the samples brittle, which leads to a decrease in impact resistance [10]. The work [11] reports on the effect of heat treatment (aging and overaging) on the fatigue life of age-hardened 15-5 PH stainless steel produced by selective laser melting. It is shown that aging leads to dispersion strengthening of the matrix, while the sensitivity to defects in the high-cycle fatigue mode increases. Overaging makes the sample ductile due to the coarsening of copper-rich precipitates and increases the amount of residual austenite.

The use of nondestructive testing methods to analyze the structure and properties of chromium-nickel steels, as well as the influence of mechanical loading and fatigue tests on them is limited to electromagnetic nondestructive testing methods: magnetic [12] and eddy current [13].

The study of the acoustic properties of steels operated under various energy force and temperature actions is a critical task, since it is the method of acoustic structuroscopy providing the most reliable connection with the structure, stress-strain state and mechanical properties of steels [14–19]. In particular, the authors proposed using the parameters of Poisson's ratio and acoustic anisotropy to assess the structural state of plastically deformed 09G2S steel [14], to assess microstructural changes during plastic deformation with subsequent heat treatment and low-cycle fatigue of 12KM8N10T austenitic steel [15; 16]. The acoustoelasticity method was used to assess residual stresses when manufacturing the axisymmetric parts from 03N17K10V10MT maraging steel [17], as well as to assess residual stresses when manufacturing rails [18]. The work [19] shows the possibility of determining the degree of damage of flat 12Kh18N10T austenitic steel samples in the region of low-cycle fatigue by the velocity of propagation of elastic waves and coercive force.

All the above-described studies in the field of acoustic structuroscopy can be implemented on specially made flat samples. In relation to round-bar samples of maraging steels, it is promising to use the non-contact electromagnetic-acoustic (EMA) method of emitting and receiving acoustic waves and the echo-shadow technique of multiple reflections due to the high accuracy and reliability of the obtained acoustic characteristics [20; 21]. This is also evidenced by the results obtained in [22; 23] dealing with assessing the influence of heat treatment and high-cycle loading by cantilever bending with rotation on the velocity of shear and Rayleigh waves in samples of 45 steel and 40H steel. One should note that martensitic steels were practically not studied previously by acoustic methods. There is also no information on the influence of heat treatment (solid solution annealing, aging) and mechanical (including cyclic) loading on the acoustic characteristics of round-bar samples used for most highly loaded parts in the oil industry.

The purpose of the work is to study the acoustic properties of samples of KhM-12 (15-5 PH) maraging steel after various types of energy impacts: heat treatment, mechanical tensile and cyclic loads.

METHODS

For the research, the authors used samples of dispersion-aging KhM-12 steel with the addition of copper (the alloy is also known as 15-5 PH and UNS S15500). The samples were subjected to various types of heat treatment:

solid solution annealing at a temperature of 1040 °C for 30 min with cooling at air and aging at temperatures of 470 and 565 °C for 3 h.

The chemical composition of 15-5 PH low-carbon steel complies with the ASTM A564 standard and contains the following alloying elements: 14 % Cr, 4 % Ni, 3 % Cu, 1 % Mn, and 1 % Si.

The samples are made in the form of cylinders with a working part diameter of 10 mm and a length of 150 mm with the fillets to a diameter of 20 mm for grippers.

The studies were carried out on a unique scientific installation "Information-measuring complex for investigation of acoustic properties of materials and products" (registration number 586308) as part of the DEMA-P information-measuring system and the DIO-1000 PA ultrasonic detector (Fig. 1). The installation provides excitation and reception of bulk transverse waves of longitudinal and radial polarization propagating along the diametric directions of the sample cross-section and a surface Rayleigh wave propagating along the sample envelope curve (Fig. 2 a). The uniqueness of the equipment is the use of a non-contact electromagnetic-acoustic method of wave emission and reception, which allows increasing significantly the reliability and accuracy of measurement results and using the EMA-transformation efficiency as an additional informative parameter. The emission and reception of a longitudinal radial-polarization wave is carried out using a flexible piezo-film such as polyvinylidene fluoride (PVDF) and a DIO-1000 PA ultrasonic detector. The installation allows recording the resulting oscillograms with a high sampling frequency and contains specific Prince IX software for calculating the main informative parameters. Typical oscillograms of the recorded series of transverse and longitudinal wave pulses re-reflected along the sample diameter are presented in Fig. 2 b, 2 c.

The velocities of longitudinal and transverse waves were calculated using the formula:

$$C_{t,l} = \frac{d \cdot n}{\Delta t},$$

where d is the average value of the object diameter at the transducer location point (determination error is 5 μm);
n is the number of analyzed reflections;
Δt is the time corresponding to n reflections.

The Rayleigh wave velocity was calculated using the formula:

$$C_R = \frac{\pi \cdot d \cdot n}{\Delta t}.$$

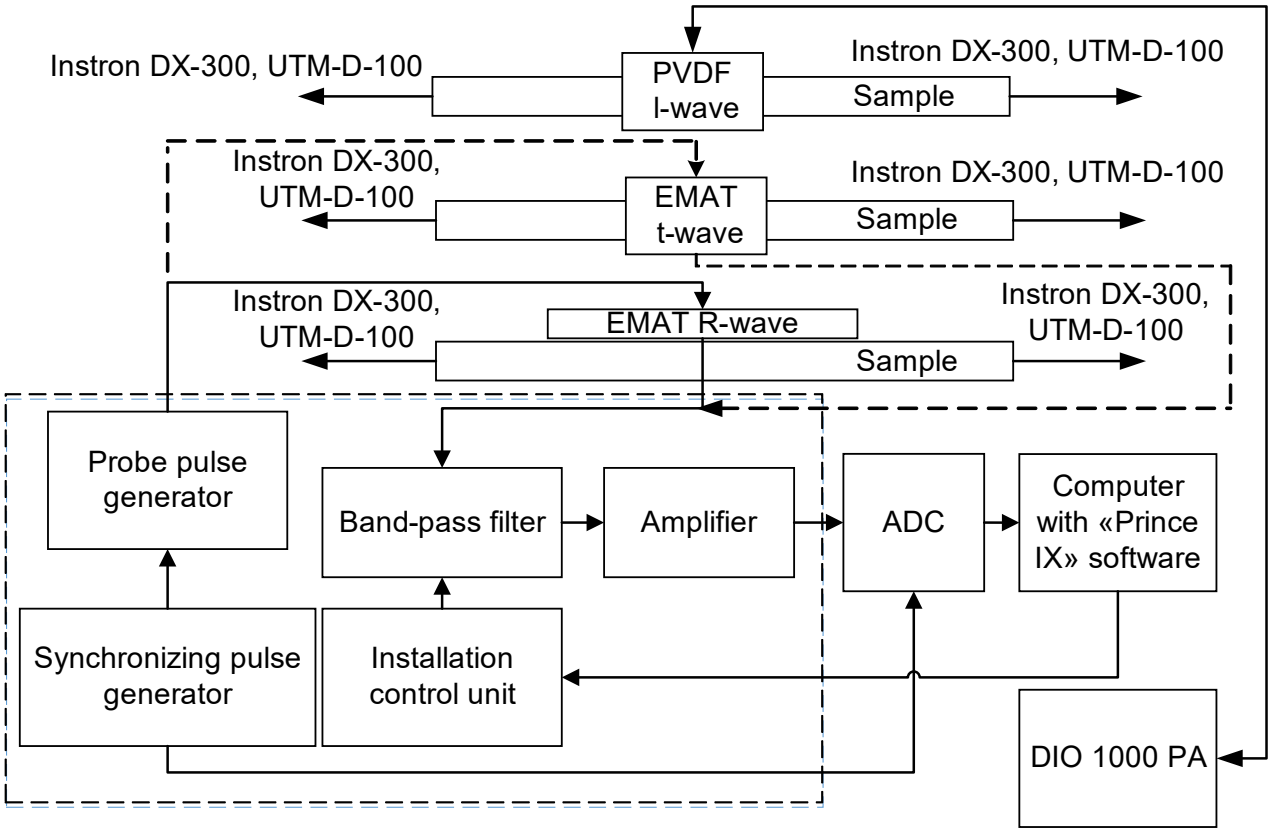

Fig. 1. *Block scheme of the experimental installation,*
where ADC is an analog-to-digital converter (LAn10-12PCI-U); SW is software;
EMAT is an electromagnetic acoustic transducer; UTM-D is a universal dynamic testing machine
Рис. 1. *Блок-схема экспериментальной установки,*
где ADC – аналого-цифровой преобразователь (ЛАн10-12PCI-У); SW – программное обеспечение;
EMAT – электромагнитно акустический преобразователь; UTM-D – универсальная испытательная машина динамическая

When determining dynamic elastic moduli (Young’s modulus E, shear modulus G, Poisson’s ratio ν), their relationship with the velocities of longitudinal and transverse waves and the material density ρ was used:

$$E = \rho \cdot C_t^2 \cdot \frac{3 - 4 \cdot C_t^2 / C_l^2}{1 - C_t^2 / C_l^2};$$

$$G = \rho \cdot C_t^2;$$

$$\nu = \frac{C_l^2 - 2 \cdot C_t^2}{2 \cdot \left(C_l^2 - C_t^2\right)}.$$

Special aspect of the acoustic method of measuring Poisson’s ratio through the velocities of elastic waves is its high accuracy determined by its independence from the sample diameter. The error in its measurements is predominant in the method of determining wave velocity.

Knowledge of the propagation velocities of transverse waves of different polarizations (axial C_{tos} and radial C_{trad}) allowed estimating the magnitude of acoustic anisotropy according to the GOST R 55805 standard:

$$A = \frac{2 \cdot \left[C_{trad} - C_{tos}\right]}{C_{trad} + C_{tos}}.$$

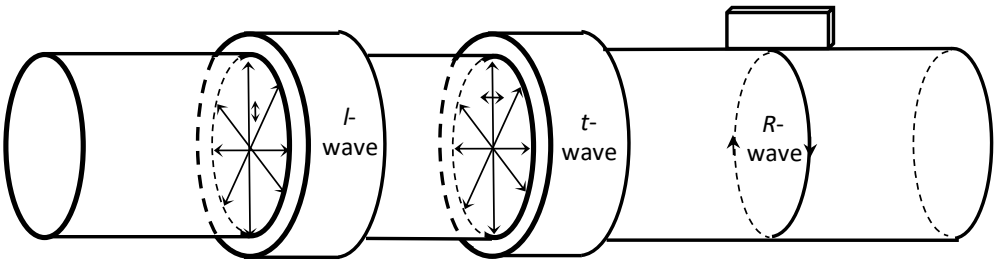

a

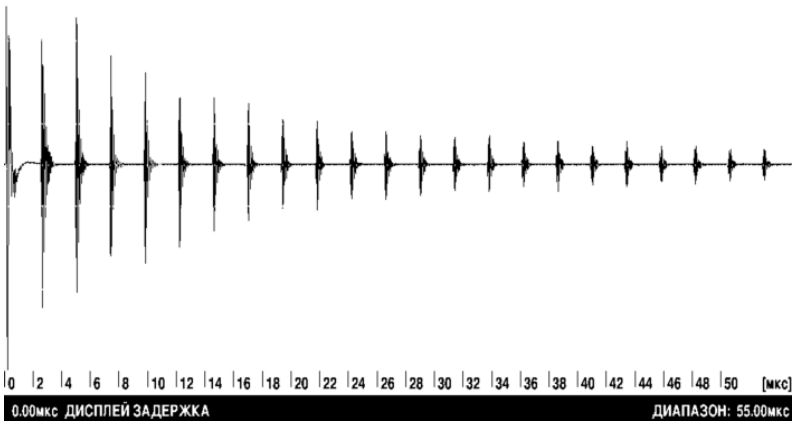

b

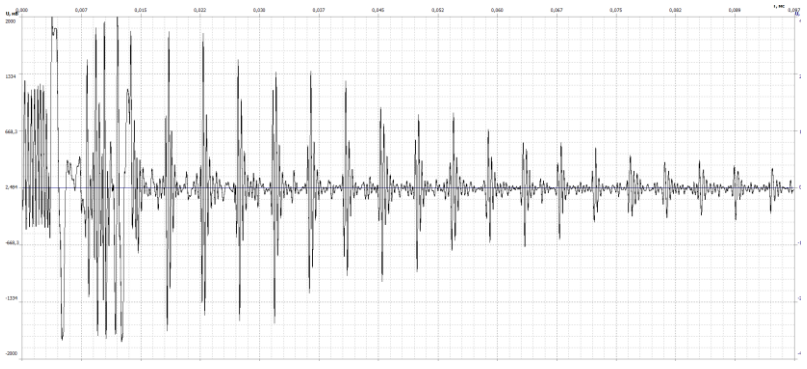

c

Fig. 2. *Scheme of propagation of bulk longitudinal l-waves, transverse t-waves and surface R-waves along the diameter of the sample (**a**); characteristic oscillograms of a series of multiple reflections of transverse waves (**b**) and longitudinal waves (**c**)*

Рис. 2. *Схема распространения объемных продольных l-волн, поперечных t-волн и поверхностных R-волн по диаметру образца (**a**); характерные осциллограммы серии многократных отражений поперечных волн (**b**) и продольных волн (**c**)*

The random error in determining the wave velocity was calculated using the formula:

$$\Delta C_r = t_{ST} \cdot \sqrt{\frac{\sum_{i=1}^{n} (C_i - C_{av})^2}{n \cdot (n-1)}},$$

where t_{ST} is the Student's coefficient (assumed equal to 2.776);
C_i is a velocity value for the i-th calculation, m/s;
C_{av} is an average velocity value based on the results of n measurements, m/s;
n is the number of measurements.

The random error in determining the velocity does not exceed 2 m/s and is comparable to the systematic error caused by the error in determining the sample diameter (5 μm) and the error in measuring time intervals (1 ns).

The EMA-transformation efficiency and the wave attenuation during propagation can be indirectly assessed by the dispersion parameter of the data array of a series of multiple reflections [24]:

$$D_x = \frac{1}{N-1} \cdot \sum_{n=0}^{N-1} (x_n - m_x)^2,$$

where N is the amount of data in the array represented as a sample sequence $\{x_n, n=0 \ldots N-1\}$;

m_x is mathematical expectation, $m_x = \frac{1}{N} \cdot \sum_{n=0}^{N-1} x_n$.

Fig. 3 shows the diagram of the physical measurement block. In addition to acoustic measurements, magnetic measurements were carried out using a KIFM-1N coercimeter (coercive force is an informative parameter), and electrical measurements were carried out using an MVP-2M eddy-current multifunctional device (relative electrical conductivity is an informative parameter). At the initial stage of the research, the density of the samples was measured by hydrostatic weighing on an HR-AG analytical balance with an accuracy of 0.5 kg/m^3.

The samples were studied in three structural states for the following loading options: the initial state (no load); with a tensile load and subsequent unloading at each step; under cyclic tension-compression load (Fig. 3).

The study of bulk wave velocity and elastic moduli of samples during uniaxial tension was carried out on an Instron DX-300 testing machine with a load increment of 10 kN and a gradual unloading in increments of 20 kN. The maximum load was 1000 MPa for the sample with solid solution annealing heat treatment, 1400 MPa for the sample aged at 470 °C, and 1200 MPa for the sample aged at 565 °C.

Studying the behavior of wave velocities during stretching allows determining the acoustoelasticity coefficient as the degree of influence of the mechanical load σ on the velocities of bulk waves:

$$k = \frac{\frac{\Delta C}{C_0}}{\sigma},$$

where k is the acoustoelastic coupling coefficient;
σ is the applied load, MPa;
$\frac{\Delta C}{C_0}$ is relative change in velocity.

The cyclic tension-compression experiment was carried out on a UIM-D-100 testing machine. A zero (pulsating) cycle with the following characteristics was used: maximum cycle stress $\sigma_{max}=\sigma$, minimum stress $\sigma_{min}=0$, average stress $\sigma_m=\sigma/2$, amplitude $\sigma_a=\sigma/2$, and asymmetry coefficient $r=0$. The maximum cycle stress was 70 % of the yield strength: for the sample after annealing – $\sigma_{max}=700$ MPa, after aging – $\sigma_{max}=1200$ MPa; cycle frequency is 5 Hz, step is from 1000 to 10 000 cycles increasing with the number of cycles.

At each step of the experimental studies, the sample average diameter was measured at control points using an MP 25 micrometer with an accuracy of 5 μm.

RESULTS

The results of studying the microstructure of the samples show that after annealing the structure is predominantly austenitic with the presence of martensite. After aging, the structure of the samples is represented by low-carbon martensite, residual austenite and a small amount of delta ferrite (0–2 %) elongated along the rolled product axis. There are precipitates of a finely dispersed structure (a strengthening phase), the amount of which determines the strength of the steel. Fig. 4 shows the 15-5 PH microstructure.

The mechanical properties of the 15-5 PH steel samples after different types of heat treatment are shown in Table 1. The results of testing the mechanical characteristics show that the strength properties and hardness of the samples after solid solution annealing are minimal. Aging at 470 °C increases strength properties and hardness to maximum values. Aging at 565 °C leads to a slight decrease in strength properties and hardness, but the highest impact strength is achieved.

Table 2 presents the physical characteristics of the samples for three heat treatment modes measured in the central region of the studied samples.

The results of acoustic structuroscopy of the 15-5 PH steel samples under various heat treatment modes (Table 2) showed:

– the minimum values of the velocities of longitudinal, transverse and Rayleigh waves, as well as elastic moduli for the 15-5 PH alloy are observed after solid solution annealing;

– Poisson's ratio, on the contrary, takes maximum values for sample No. 1 and minimum values for sample No. 3;

– wave velocities increase after aging due to the solid solution decomposition with the release of copper deposits, as well as the release of chromium and silicon from the solid solution;

– acoustic anisotropy of properties is more significant for sample No. 1 and decreases by more than twice for samples No. 2 and 3.

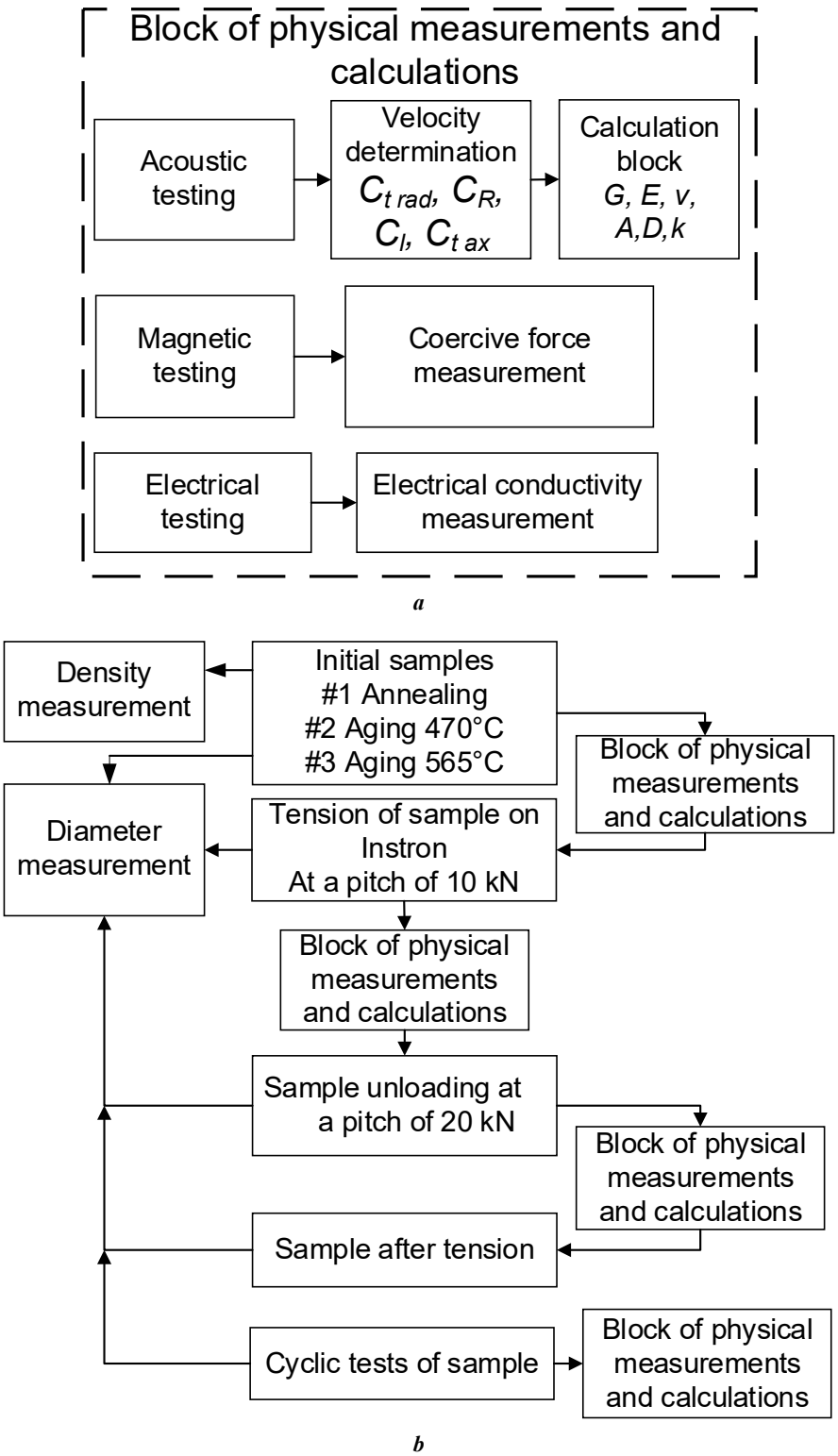

Fig. 3. *Diagram of physical measurement block (**a**); diagram of block of tests during loading (**b**)*
Рис. 3. *Схема блока физических измерений (**a**); схема блока испытаний в процессе нагружения (**b**)*

Fig. 5 shows the distribution of Poisson's ratio and anisotropy coefficient along the length of the studied samples after heat treatment.

Changes in the wave velocity and Poisson's ratio when stretching the samples lead to a smooth linear decrease in the velocity of the transverse axial-polarization wave over the entire range of applied loads (Fig. 6).

The tension-compression influence on the relative change in the rate of cyclic loading is presented in Fig. 7. The nature of the curves is nonlinear.

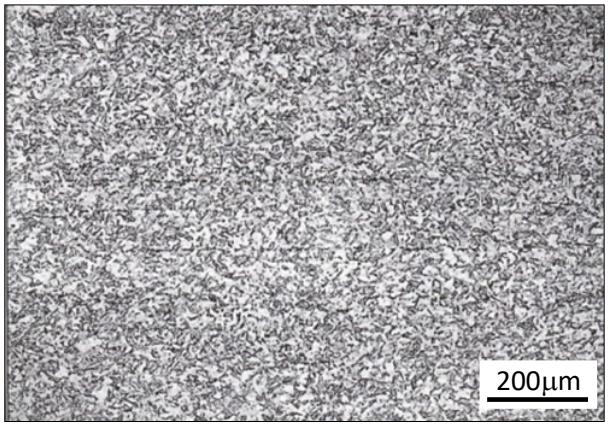

Fig. 4. *Microstructure of the 15-5 PH steel after aging*
Рис. 4. *Микроструктура стали ХМ-12 после старения*

Table 1. *Mechanical properties of the 15-5 PH steel after various types of heat treatment*
Таблица 1. *Механические свойства стали ХМ-12 после различных термических обработок*

Type and mode of heat treatment	Solid solution annealing at 1040 °C, 0.5 h in the air	Aging at 470 °C, 3 h	Aging at 565 °C, 3 h
	Sample No.		
	1	2	3
Tensile strength σ_{UTS}, MPa	1 070	1 455	1 230
Yield strength $\sigma_{0.2}$, MPa	990	1 420	1 200
Percentage elongation, %	13.5	12.5	12.5
Percentage reduction, %	67	60	65
Impact strength KCU, J/cm^2	168	110	190
Hardness, HRC	30	45	39

DISCUSSION

The data in Table 2 show that with increasing aging temperature, the steel structure becomes ordered with the appearance of new phases [3], and the size of the copper-enriched phase increases. According to [5], the microstructure of steel during long-term aging undergoes a complex evolution, including the development of a minor austenitic phase, copper-rich deposits, as well as the release of chromium and silicon from the solid solution.

Electrical conductivity decreases relative to solid solution annealing after aging at 470 °C, and at 565 °C, it increases to values corresponding to annealing. The coercive force relative to solid solution annealing increases slightly after aging at 470 °C. An increase in the aging temperature to 565 °C leads to a decrease in coercive force values, which may be associated with a decrease in internal stresses caused by the crystal lattice distortion. This is confirmed in [25], which shows that the coercive force of a maraging iron-chromium-nickel alloy depends on the structure morphology, stresses, grain size, and shape.

From the analysis of Fig. 5 and 6 it is clear that, despite the change in Poisson's ratio within a very small range (no more than 0.25 %), there are significant differences in the acoustic anisotropy coefficient along the length of the sample, which indicates the presence of heterogeneity in the sample. The most significant deviation in velocity is 0.96 % for sample No. 2 after aging at 470 °C; the least significant is 0.67 % for sample No. 3 after aging at 565 °C. The high sensitivity of transverse waves to tensile loads is explained by the coincidence of the axial direction of wave polarization with the force direction. The velocity of a longitudinal wave polarized across the direction of tensile stresses practically does not change (changes are within the error). The corresponding calculated coefficients of the studied samples are presented in Table 3.

One should note that during the stretching process, an increase in the EMA-transformation efficiency is observed

Table 2. *Physical characteristics of the 15-5 PH steel samples before loading*
Таблица 2. *Физические характеристики образцов стали ХМ-12 до нагружения*

Physical characteristic	Heat treatment modes		
	Annealing	Aging at 470 °C	Aging at 565 °C
Wave velocity C_l, m/s	5 798	5 838	5 866
Wave velocity C_{trad}, m/s	3 136	3 154	3 192
Wave velocity C_{tos}, m/s	3 123	3 150	3 186
Wave velocity C_R, m/s	2 907	2 922	2 956
Density ρ, kg/m^3	7 687	7 677	7 689
Young’s modulus E, GPa	194.6	200.0	202.7
Shear modulus G, GPa	75.2	77.4	78.4
Poisson’s ratio ν	0.2947	0.2913	0.2896
Electrical conductivity, mkV	3 860	3 907	3 947
Coercive force, A/cm	23.2	17.5	17.1
Anisotropy coefficient, %	0.417	0.127	0.208
Dispersion, mV^2	6 755	6 851	6 371

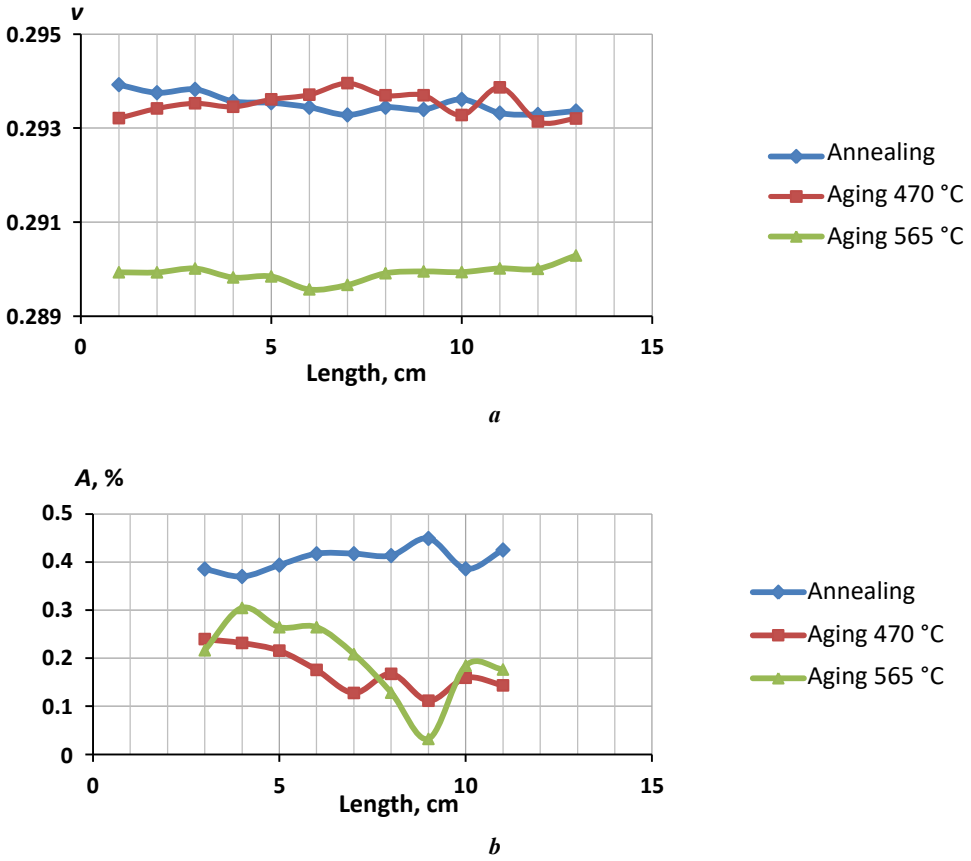

Fig. 5. *Distribution of Poisson’s ratio* ***(a)*** *and acoustic anisotropy coefficient* ***(b)*** *along the length of samples subjected to various heat treatment modes*
Рис. 5. *Распределение коэффициента Пуассона* ***(а)*** *и коэффициента акустической анизотропии* ***(b)*** *по длине образцов, подвергнутых различным режимам термообработки*

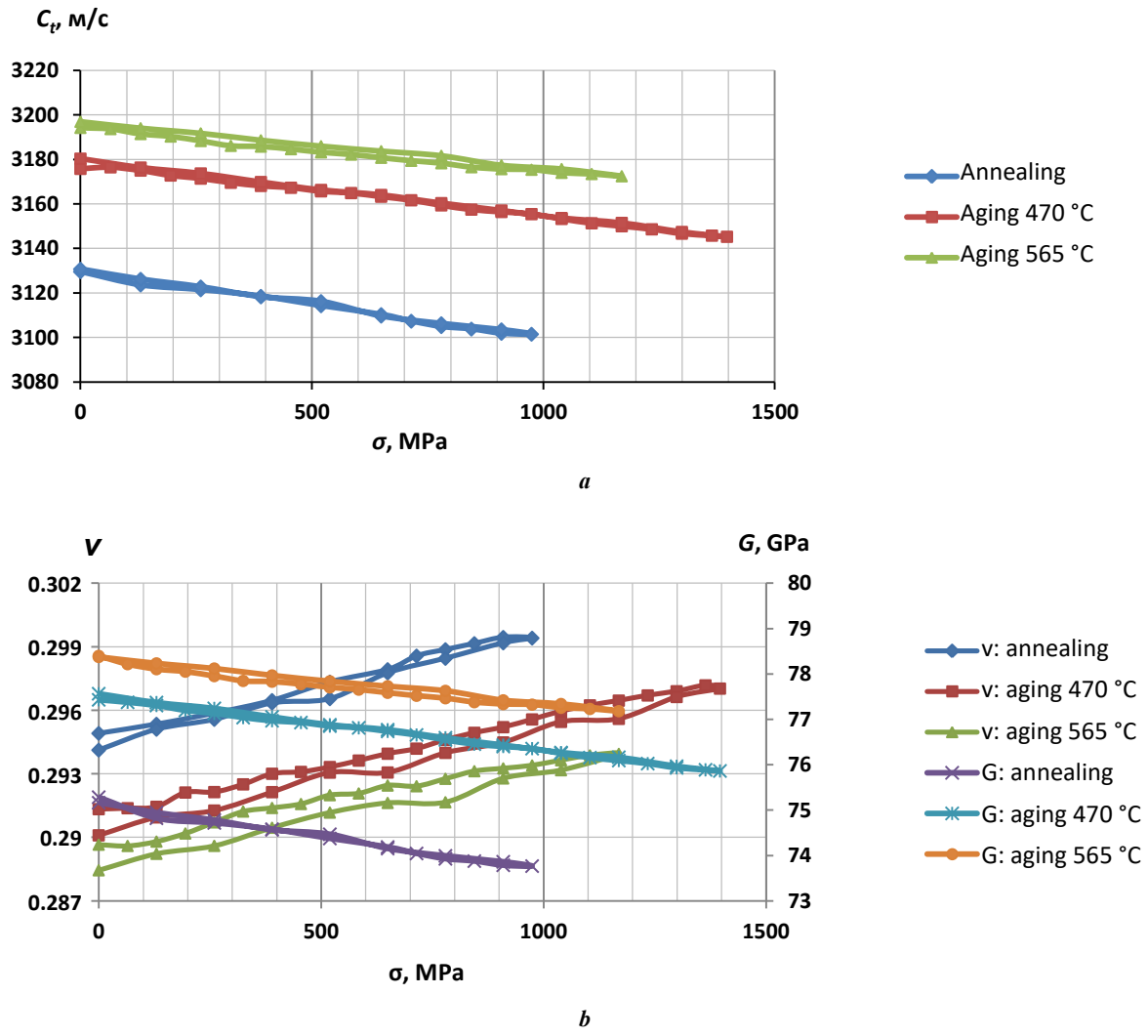

Fig. 6. *Change in the transverse wave velocity (**a**), shear elastic modulus and Poisson's ratio (**b**) during tension process*
Рис. 6. *Изменение скорости поперечной волны (**a**), упругого модуля сдвига и коэффициента Пуассона (**b**) в процессе растяжения*

(Fig. 8). It is nonlinear in nature: a slow increase at low loads, a sharper increase at loads approaching the yield strength of the material. In the area of high loads, a decrease in the EMA-transformation coefficient is observed, which is explained by a decrease in the sample radius near the yield point, and, consequently, an increase in the gap between the EMA transducer and the test object, which leads to a decrease in eddy currents in the sample surface layer. Other things being equal, the EMA-transformation coefficient has a maximum value for sample No. 2 (aging at 470 °C) (Table 3) and correlates with the maximum values of sample hardness (Table 1) and maximum coercive force (Table 2), which corresponds to conventional beliefs about the influence of the material magnetic properties on the EMA-transformation efficiency.

After unloading, virtually no changes in the velocities of the acoustic waves are observed. At the same time, electrical conductivity increases significantly for all types of heat treatment.

The linear decrease in the relative change in the transverse wave velocity (Fig. 7) to 0.32 % for the sample after annealing and to 0.14 % for the sample after aging observed at the initial stage (10 cycles) is a consequence of preloading the sample (up to 359 MPa for the sample after annealing and up to 490 MPa for the sample after aging) and corresponds to the value obtained under static uniaxial tension. For a sample after annealing, a subsequent increase in the number of cycles leads to a less significant decrease in the transverse wave velocity and further stabilization of the values in the region of 1000 cycles and above. Changes in velocity with a number of cycles greater than 1000 are within the measurement error and primarily determined by small temperature fluctuations. For the sample after aging, a similar pattern is observed with a more nonlinear curve nature. One should note that with a small number of cycles, there is a slight (in comparison with the transverse wave) increase in the longitudinal wave velocity, followed by its decrease with a large number of cycles. The indicated differences in the behavior of longitudinal and transverse waves lead to changes in the elastic moduli during the cyclic tests presented in Fig. 7 b, 7 c as the loading cycles increase.

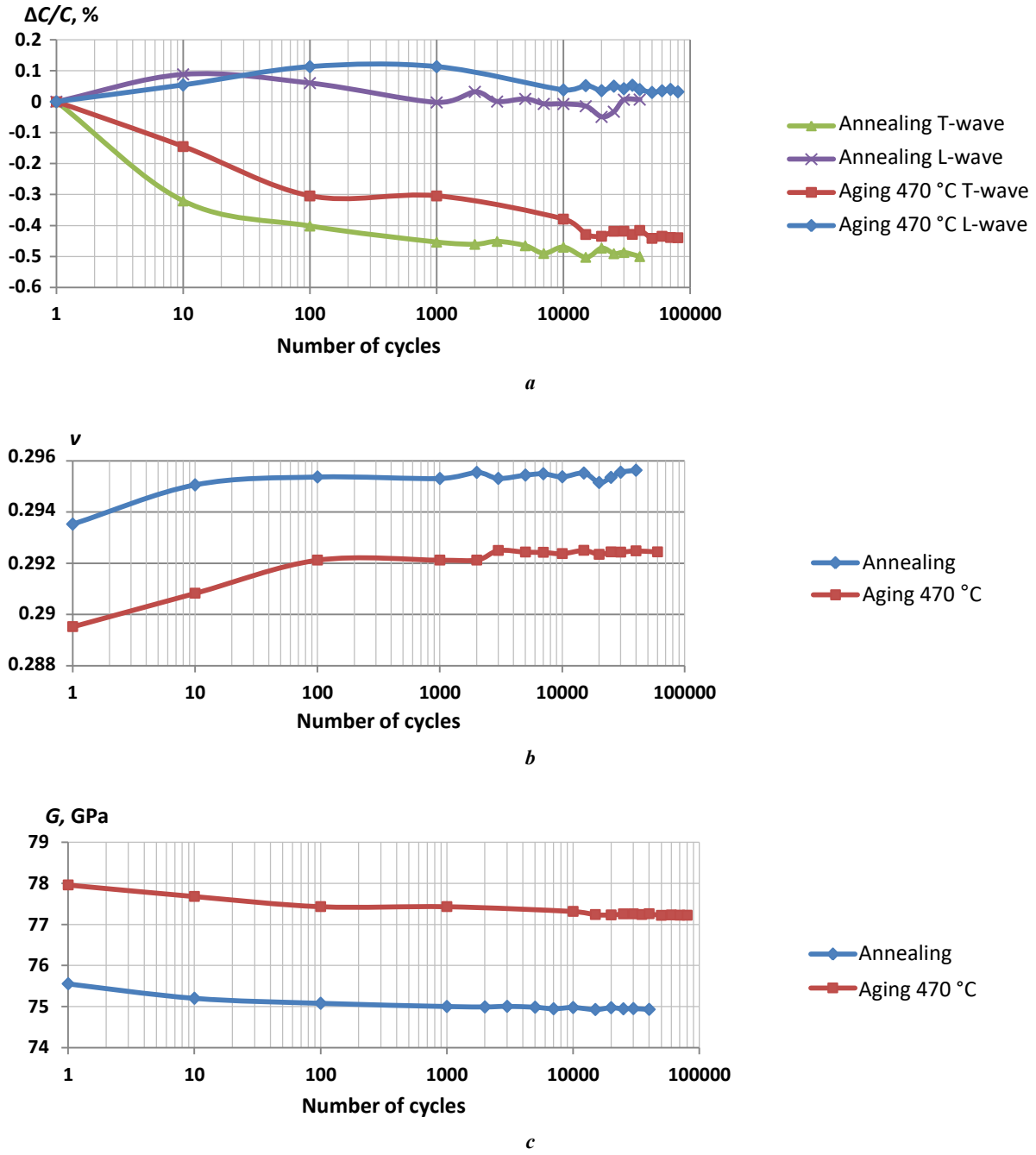

Fig. 7. *Change in bulk wave velocity (**a**), shear modulus (**b**), and Poisson’s ratio (**c**) depending on the number of tension-compression cycles*
Рис. 7. *Изменение скоростей объемных волн (**a**), модуля сдвига (**b**) и коэффициента Пуассона (**c**) от количества циклов растяжения-сжатия*

Table 3. *Acoustoelasticity coefficients and EMA-transformation coefficient of the studied samples*
Таблица 3. *Коэффициенты акустоупругости и коэффициента ЭМА-преобразования исследованных образцов*

Characteristic	Heat treatment mode		
	Annealing	Aging at 470 °C	Aging at 565 °C
Acoustoelasticity coefficient, k, TPa^{-1}	−9.2	−6.9	−5.7
EMA-transformation coefficient, K_{EMA}, mV	966	1 128	666

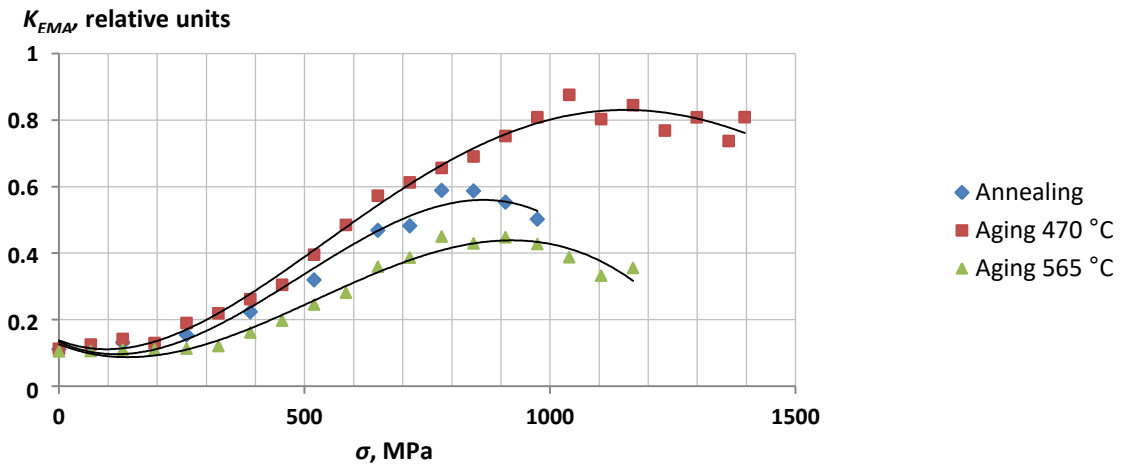

Fig. 8. *Change in relative EMA-transformation coefficient in the process of tension*
Рис. 8. *Изменение относительного коэффициента ЭМА-преобразования в процессе растяжения*

One should note that a further increase in the number of cycles to $4 \cdot 10^5$ and an increase in the loading amplitude to 0.8 of the yield strength did not lead to the destruction of any of the samples. Considering that the process of nucleation and accumulation of microcracks should lead to a decrease in velocity with increasing load [19; 22], one can assume that it is not decisive in the behavior of these curves. Probably, the stabilization of the behavior of the curves during loading is determined by the appearance in the 15-5 PH steel microstructure of the strain martensite hardening phase characteristic of these materials, which can replace residual austenite.

CONCLUSIONS

The study of the acoustic characteristics of KhM-12 (15-5 PH) maraging steel samples after heat treatment of solid solution annealing and subsequent aging under mechanical tensile and cyclic loads showed the presence of the following structure-sensitive parameters: transverse axial-polarization wave velocity, elastic shear modulus, Poisson's ratio, acoustic anisotropy coefficient, acoustoelasticity coefficient, double electromagnetic-acoustic transformation, electrical conductivity and coercive force coefficients.

It was found that the minimum values of the velocities of longitudinal, transverse and Rayleigh waves for the KhM-12 (15-5 PH) alloy are observed after solid solution annealing. The velocity of a transverse wave with polarization in the direction of the force in the elastic region of mechanical loading decreases in direct proportion to the load, while the maximum value of the acoustoelastic coefficient corresponds to the sample after annealing (-9.2 TPa^{-1}). Young's and shear moduli decrease linearly, while Poisson's ratio, on the contrary, increases linearly in the range of loads under study. Increasing the number of cycles leads to a decrease in the transverse wave velocity in the range of up to 1000 cycles and further stabilization of values in the region of higher values.

The non-contact acoustic echo-shadow method developed for research based on multiple reflections and the equipment implementing it using non-contact EMA principles of excitation and reception of waves can be effectively used for tasks of acoustic structuroscopy, when assessing the stress-strain state, in cyclic tests and other types of impacts for a wide class of metals and alloys with special properties.

REFERENCES

1. Eremin E.N., Losev A.S., Ponomarev I.A., Borodikhin S.A. Thermal treatment impact upon structure, properties and phase structure of steel 10G7M3S2AFTYU weld with powder wire. *Science intensive technologies in mechanical engineering*, 2020, no. 5, pp. 3–8. DOI: 10.30987/2223-4608-2020-5-3-8.
2. Gromov V.I., Yakusheva N.A., Polunov I.L. Evaluation of the effect of heat treatment on mechanical properties of maraging steels in the alloying system Fe–Ni–Mo–Ti–Al. *Trudy VIAM (Proceedings of VIAM)*, 2017, no. 11, pp. 12–20. DOI: 10.18577/2307-6046-2017-0-11-2-2.
3. Couturier L., De Geuser F., Deschamps A. Microstructural evolution during long time aging of 15–5PH stainless steel. *Materialia*, 2020, vol. 9, article number 100634. DOI: 10.1016/j.mtla.2020.100634.
4. Niu Jingpeng, Cui Bing, Jin Huijin, Yan Jialing, Meng Wei, Min Chunying, Xu Dong. Effect of Post-Weld Aging Temperature on Microstructure and Mechanical Properties of Weld Metal of 15-5 PH. *Journal of Materials Engineering and Performance*, 2020, vol. 29, pp. 7026–7033. DOI: 10.1007/s11665-020-05193-y.
5. Jin Chunhui, Zhou Honglin, Lai Yuan, Li Bei, Zhang Kewei, Chen Huiqin Zhao Jinhua. Microstructure and mechanical properties of 15-5 PH stainless steel under different aging temperature. *Metallurgical Research and Technology*, 2021, vol. 118, no. 6, article number 601. DOI: 10.1051/metal/2021078.

6. Valiorgue F., Zmelty V., Dumas M., Chomienne V., Verdu C., Lefebvre F., Rech J. Influence of residual stress profile and surface microstructure on fatigue life of a 15-5PH. *Procedia Engineering*, 2018, vol. 213, pp. 623–629. DOI: 10.1016/j.proeng.2018.02.058.
7. Zhou Tao, Faleskog J., Babu R.P., Odqvist J., Yu Hao, Hedström P. Exploring the relationship between the microstructure and strength of fresh and tempered martensite in a maraging stainless steel Fe–15Cr–5Ni. *Materials Science and Engineering: A*, 2019, vol. 745, pp. 420–428. DOI: 10.1016/j.msea.2018.12.126.
8. Avula I., Arohi A.Ch., Kumar Ch.S., Sen I. Microstructure, Corrosion and Mechanical Behavior of 15-5 PH Stainless Steel Processed by Direct Metal Laser Sintering. *Journal of Materials Engineering and Performance*, 2021, vol. 30, pp. 6924–6937. DOI: 10.1007/s11665-021-06069-5.
9. Nong X.D., Zhou X.L., Li J.H., Wang Y.D., Zhao Y.F., Brochu M. Selective laser melting and heat treatment of precipitation hardening stainless steel with a refined microstructure and excellent mechanical properties. *Scripta Materialia*, 2020, vol. 178, pp. 7–12. DOI: 10.1016/j.scriptamat.2019.10.040.
10. Sarkar S., Mukherjee S., Kumar Ch.S., Nath A.K. Effects of heat treatment on microstructure, mechanical and corrosion properties of 15-5 PH stainless steel parts built by selective laser melting process. *Journal of Manufacturing Processes*, 2020, vol. 150, pp. 279–294. DOI: 10.1016/j.jmapro.2019.12.048.
11. Sarkar S., Kumar Ch.S., Nath A.K. Effects of heat treatment and build orientations on the fatigue life of selective laser melted 15-5 PH stainless steel. *Materials Science and Engineering: A*, 2019, vol. 755, pp. 235–245. DOI: 10.1016/j.msea.2019.04.003.
12. Gorkunov E.S., Povolotskaya A.M., Zadvorkin S.M., Putilova E.A., Mushnikov A.N., Bazulin E.G., Vopilkin A.K. Some features in the behavior of magnetic and acoustic characteristics of hot-rolled 08G2B steel under cyclic loading. *Russian Journal of Nondestructive Testing*, 2019, vol. 55, no. 11, pp. 827–836. DOI: 10.1134/S0130308219110034.
13. Takeda S., Uchimoto T., Kita A., Matsumoto T., Sasaki T. Mechanism study of the residual stress evaluation of low-carbon steels using the eddy current magnetic signature method. *Journal of Magnetism and Magnetic Materials*, 2021, vol. 538, article number 168268. DOI: 10.1016/j.jmmm.2021.168268.
14. Mishakin V.V., Gonchar A.V., Klyushnikov V.A., Kurashkin K.V. Study of the effect of plastic deformation on the crystallographic texture and acoustic characteristics of low-alloy steel. *Problems of Strength and Plasticity / Problemy prochnosti i plastichnosti*, 2021, vol. 83, no. 3, pp. 255–264. DOI: 10.32326/1814-9146-2021-83-3-255-264.
15. Gonchar A.V., Klyushnikov V.A., Mishakin V.V. The effect of plastic deformation and subsequent heat treatment on the acoustic and magnetic properties of 12Khl8N10T steel. *Industrial laboratory. Diagnostics of materials*, 2019, vol. 85, no. 2, pp. 23–28. DOI: 10.26896/1028-6861-2019-85-2-23-28.
16. Mishakin V.V., Gonchar A.V., Kurashkin K.V., Klyushnikov V.A., Kachanov M. On low-cycle fatigue of austenitic steel. Part I: Changes of Poisson’s ratio and elastic anisotropy. *International Journal of Engineering Science*, 2021, vol. 168, article number 103567. DOI: 10.1016/j.ijengsci.2021.103567.
17. Uglov A.L., Khlybov A.A., Bychkov A.L., Kuvshinov M.O. About Non-Destructive Control of Residual Stresses in Axisymmetric Parts Made of Steel 03Ni17Co10W10MoTi. *Vestnik IzhGTU imeni M.T. Kalashnikova*, 2019, vol. 22, no. 4, pp. 3–9. DOI: 10.22213/2413-1172-2019-4-3-9.
18. Muravev V.V., Lenkov S.V., Tapkov K.A. In-production nondestructive testing of internal stresses in rails using acoustoelasticity method. *Russian Journal of Nondestructive Testing*, 2019, vol. 55, no. 1, pp. 8–14. DOI: 10.1134/S01303082190100020.
19. Khlybov A.A., Kabaldin Yu.G., Ryabov D.A., Anosov M.S., Shagatin D.A. Study of the damage to 12Cr18Ni10Ti steel samples under low cycle fatigue using methods of nondestructive control. *Industrial laboratory. Diagnostics of materials*, 2021, vol. 87, no. 5, pp. 61–67. DOI: 10.26896/1028-6861-2021-87-5-61-67.
20. Muraveva O.V., Muravev V.V., Basharova A.F., Sintsov M.A., Bogdan O.P. Thermal treatment effect and structural state of rod-shaped assortment 40Kh steel on the speed of ultrasound waves and poisson coefficient. *Steel in Translation*, 2020, vol. 50, no. 8, pp. 579–584. EDN: MKTWDN.
21. Muravev V.V., Muraveva O.V., Vagapov T.R., Makarova V.E., Stepanova E.A. Acoustic and electromagnetic properties of civilian gun blanks. *Intelligent Systems in Manufacturing*, 2023, vol. 21, no. 1, pp. 59–70. EDN: KBBVGW.
22. Muravev V.V., Budrin A.Yu., Sintsov M.A. Influence of high-cycle fatigue on the speed of shear and Rayleigh waves in steel bars of different heat treatment. *Intelligent Systems in Manufacturing*, 2020, vol. 18, no. 4, pp. 4–10. DOI: 10.22213/2410-9304-2020-4-10.
23. Muravev V.V., Budrin A.Yu., Sintsov M.A. Structuroscopy of heat-treated steel bars by the speed of propagation of Rayleigh waves. *Intelligent Systems in Manufacturing*, 2020, vol. 18, no. 2, pp. 37–43. DOI: 10.22213/2410-9304-2020-2-37-43.
24. Muraveva O.V., Brester A.F., Muravev V.V. Comparative sensitivity of informative parameters of electromagnetic-acoustic mirror-shadow multiple reflections method during bar stock testing. *Russian Journal of Nondestructive Testing*, 2022, vol. 58, no. 8, pp. 689–704. EDN: BQEKGO.
25. Kazantseva N.V., Merkushev A.G., Shishkin D.A., Ezhov I.V., Davidov D.I., Rigmant M.B., Terentev P.B., Egorova L.Yu. Magnetic Properties and Structure of Products from 1.4540 Stainless Steel Manufactured by 3D Printing. *Physics of Metals and Metallography*, 2019, vol. 120, pp. 1270–1275. DOI: 10.1134/S0031918X19130118.

СПИСОК ЛИТЕРАТУРЫ

1. Еремин Е.Н., Лосев А.С., Пономарев И.А., Бородихин С.А. Влияние режимов термической обработки на структуру, свойства и фазовый состав стали 10Г7М3С2АФТЮ, наплавленной порошковой проволокой // Наукоемкие технологии в машиностроении. 2020. № 5. С. 3–8. DOI: 10.30987/2223-4608-2020-5-3-8.

2. Громов В.И., Якушева Н.А., Полунов И.Л. Оценка влияния режимов термической обработки на уровень механических свойств мартенситостареющих сталей системы легирования Fe–Ni–Mo–Ti–Al // Труды ВИАМ. 2017. № 11. С. 12–20. DOI: 10.18577/2307-6046-2017-0-11-2-2.
3. Couturier L., De Geuser F., Deschamps A. Microstructural evolution during long time aging of 15–5PH stainless steel // Materialia. 2020. Vol. 9. Article number 100634. DOI: 10.1016/j.mtla.2020.100634.
4. Niu Jingpeng, Cui Bing, Jin Huijin, Yan Jialing, Meng Wei, Min Chunying, Xu Dong. Effect of Post-Weld Aging Temperature on Microstructure and Mechanical Properties of Weld Metal of 15-5 PH // Journal of Materials Engineering and Performance. 2020. Vol. 29. P. 7026–7033. DOI: 10.1007/s11665-020-05193-y.
5. Jin Chunhui, Zhou Honglin, Lai Yuan, Li Bei, Zhang Kewei, Chen Huiqin, Zhao Jinhua. Microstructure and mechanical properties of 15-5 PH stainless steel under different aging temperature // Metallurgical Research and Technology. 2021. Vol. 118. № 6. Article number 601. DOI: 10.1051/metal/2021078.
6. Valiorgue F., Zmelty V., Dumas M., Chomienne V., Verdu C., Lefebvre F., Rech J. Influence of residual stress profile and surface microstructure on fatigue life of a 15-5PH // Procedia Engineering. 2018. Vol. 213. P. 623–629. DOI: 10.1016/j.proeng.2018.02.058.
7. Zhou Tao, Faleskog J., Babu R.P., Odqvist J., Yu Hao, Hedström P. Exploring the relationship between the microstructure and strength of fresh and tempered martensite in a maraging stainless steel Fe–15Cr–5Ni // Materials Science and Engineering: A. 2019. Vol. 745. P. 420–428. DOI: 10.1016/j.msea.2018.12.126.
8. Avula I., Arohi A.Ch., Kumar Ch.S., Sen I. Microstructure, Corrosion and Mechanical Behavior of 15-5 PH Stainless Steel Processed by Direct Metal Laser Sintering // Journal of Materials Engineering and Performance. 2021. Vol. 30. P. 6924–6937. DOI: 10.1007/s11665-021-06069-5.
9. Nong X.D., Zhou X.L., Li J.H., Wang Y.D., Zhao Y.F., Brochu M. Selective laser melting and heat treatment of precipitation hardening stainless steel with a refined microstructure and excellent mechanical properties // Scripta Materialia. 2020. Vol. 178. P. 7–12. DOI: 10.1016/j.scriptamat.2019.10.040.
10. Sarkar S., Mukherjee S., Kumar Ch.S., Nath A.K. Effects of heat treatment on microstructure, mechanical and corrosion properties of 15-5 PH stainless steel parts built by selective laser melting process // Journal of Manufacturing Processes. 2020. Vol. 150. P. 279–294. DOI: 10.1016/j.jmapro.2019.12.048.
11. Sarkar S., Kumar Ch.S., Nath A.K. Effects of heat treatment and build orientations on the fatigue life of selective laser melted 15-5 PH stainless steel // Materials Science and Engineering: A. 2019. Vol. 755. P. 235–245. DOI: 10.1016/j.msea.2019.04.003.
12. Горкунов Э.С., Поволоцкая А.М., Задворкин С.М., Путилова Е.А., Мушников А.Н., Базулин Е.Г., Вопилкин А.Х. Особенности поведения магнитных и акустических характеристик горячекатаной стали 08Г2Б при циклическом нагружении // Дефектоскопия. 2019. № 11. С. 21–31. DOI: 10.1134/S0130308219110034.
13. Takeda S., Uchimoto T., Kita A., Matsumoto T., Sasaki T. Mechanism study of the residual stress evaluation of low-carbon steels using the eddy current magnetic signature method // Journal of Magnetism and Magnetic Materials. 2021. Vol. 538. Article number 168268. DOI: 10.1016/j.jmmm.2021.168268.
14. Мишакин В.В., Гончар А.В., Клюшников В.А., Курашкин К.В. Исследование влияния пластического деформирования на кристаллографическую текстуру и ультразвуковые характеристики низколегированной стали // Проблемы прочности и пластичности. 2021. Т. 83. № 3. С. 255–264. DOI: 10.32326/1814-9146-2021-83-3-255-264.
15. Гончар А.В., Клюшников В.А., Мишакин В.В. Влияние пластического деформирования и последующей термообработки на акустические и электромагнитные свойства стали 12Х18Н10Т // Заводская лаборатория. Диагностика материалов. 2019. Т. 85. № 2. С. 23–28. DOI: 10.26896/1028-6861-2019-85-2-23-28.
16. Mishakin V.V., Gonchar A.V., Kurashkin K.V., Klyushnikov V.A., Kachanov M. On low-cycle fatigue of austenitic steel. Part I: Changes of Poisson’s ratio and elastic anisotropy // International Journal of Engineering Science. 2021. Vol. 168. Article number 103567. DOI: 10.1016/j.ijengsci.2021.103567.
17. Углов А.Л., Хлыбов А.А., Бычков А.Л., Кувшинов М.О. О неразрушающем контроле остаточных напряжений в деталях осесимметричной формы из стали 03Н17К10В10МТ // Вестник ИжГТУ имени М.Т. Калашникова. 2019. Т. 22. № 4. С. 3–9. DOI: 10.22213/2413-1172-2019-4-3-9.
18. Муравьев В.В., Тапков К.А., Леньков С.В. Неразрушающий контроль внутренних напряжений в рельсах при изготовлении с использованием метода акустоупругости // Дефектоскопия. 2019. № 1. С. 10–16. DOI: 10.1134/S0130308219010020.
19. Хлыбов А.А., Кабалдин Ю.Г., Рябов Д.А., Аносов М.С., Шагатин Д.А. Исследование поврежденности образцов из стали 12Х18Н10Т при малоцикловой усталости методами неразрушающего контроля // Заводская лаборатория. Диагностика материалов. 2021. Т. 87. № 5. С. 61–67. DOI: 10.26896/1028-6861-2021-87-5-61-67.
20. Муравьева О.В., Муравьев В.В., Башарова А.Ф., Синцов М.А., Богдан О.П. Влияние термической обработки и структурного состояния стали 40Х прутkового сортамента на скорость ультразвуковых волн и коэффициент Пуассона // Сталь. 2020. № 8. С. 63–68. EDN: MKTWDN.
21. Муравьев В.В., Муравьева О.В., Вагапов Т.Р., Макарова В.Е., Степанова Е.А. Акустические и электромагнитные свойства заготовок стволов гражданских ружей // Интеллектуальные системы в производстве. 2023. Т. 21. № 1. С. 59–70. EDN: KBBVGW.
22. Муравьев В.В., Будрин А.Ю., Синцов М.А. Влияние циклически изменяющихся нагрузок на скорости сдвиговых и рэлеевских волн в стальных прутках разной термической обработки // Интеллектуальные системы в производстве. 2020. Т. 18. № 4. С. 4–10. DOI: 10.22213/2410-9304-2020-4-10.
23. Муравьев В.В., Будрин А.Ю., Синцов М.А. Структуроскопия термически обработанных стальных

прутков по скорости распространения рэлеевских волн // Интеллектуальные системы в производстве. 2020. Т. 18. № 2. С. 37–43. DOI: 10.22213/2410-9304-2020-2-37-43.
24. Муравьева О.В., Брестер А.Ф., Муравьев В.В. Сравнительная чувствительность информативных параметров электромагнитно-акустического зеркально-теневого метода на многократных отражениях при контроле пруткового проката // Дефектоскопия. 2022. № 8. С. 36–51. EDN: BQEKGO.
25. Kazantseva N.V., Merkushev A.G., Shishkin D.A., Ezhov I.V., Davidov D.I., Rigmant M.B., Terentev P.B., Egorova L.Yu. Magnetic Properties and Structure of Products from 1.4540 Stainless Steel Manufactured by 3D Printing // Physics of Metals and Metallography. 2019. Vol. 120. P. 1270–1275. DOI: 10.1134/S0031918X19130118.

Акустические свойства мартенситно-стареющей стали ХМ-12 после энергетических воздействий

Муравьева Ольга Владимировна[1,2,3], доктор технических наук, профессор,
профессор кафедры «Приборы и методы измерений, контроля, диагностики»
Муравьев Виталий Васильевич[1,2,4], доктор технических наук, профессор,
профессор кафедры «Приборы и методы измерений, контроля, диагностики»
Волкова Людмила Владимировна[1,5], кандидат технических наук, доцент,
доцент кафедры «Приборы и методы измерений, контроля, диагностики»
Владыкин Алексей Леонидович*[1,6], аспирант
Белослудцев Константин Юрьевич[1], магистрант
[1]*Ижевский государственный технический университет имени М.Т. Калашникова, Ижевск (Россия)*
[2]*Удмуртский федеральный исследовательский центр Уральского отделения РАН, Ижевск (Россия)*

***E-mail:** pmkk@istu.ru, vladykin-ndt@mail.ru

[3]ORCID: https://orcid.org/0000-0003-3442-8163
[4]ORCID: https://orcid.org/0000-0001-8590-1382
[5]ORCID: https://orcid.org/0000-0001-5128-6465
[6]ORCID: https://orcid.org/0009-0006-1813-2011

Поступила в редакцию 05.07.2023 *Принята к публикации 28.11.2023*

Аннотация: Исследование акустических свойств мартенситно-стареющих сталей, эксплуатируемых в условиях различных энергетических силовых и температурных воздействий, является актуальной задачей, так как именно метод акустической структуроскопии обеспечивает наиболее достоверную связь со структурой, напряженно-деформированным состоянием и механическими свойствами сталей. Работа посвящена исследованию акустических свойств образцов мартенситно-стареющей стали ХМ-12 при различных термических обработках в условиях механических растягивающих и циклических нагрузок. Исследованы образцы мартенситно-стареющей стали ХМ-12 в трех структурных состояниях: после отжига на твердый раствор и последующего старения при 470 и 565 °С; при испытаниях на растяжение; в процессе циклической нагрузки растяжения-сжатия. В исследованиях использована уникальная научная установка «Информационно-измерительный комплекс для исследований акустических свойств материалов и изделий». Она реализует акустический зеркально-теневой метод на многократных отражениях с применением электромагнитно-акустического и пьезоэлектрического преобразователей на основе поливинилиденфторидной пленки для возбуждения и приема волн и позволяет определить скорости распространения волн с погрешностью не более 2 м/с. Исследованы акустические (скорость волн, упругие модули, коэффициенты электромагнитно-акустического (ЭМА) преобразования, коэффициенты акустической анизотропии, коэффициенты акустоупругой связи) и электромагнитные (коэрцитивная сила и электропроводность) характеристики образцов: в исходном состоянии (до нагружения); пошагово в процессе растягивающих нагрузок и последующего разгружения; после испытаний на растяжение; в процессе циклической нагрузки растяжения-сжатия. Выявлено, что наибольшей структурной чувствительностью к механической растягивающей нагрузке и циклическому нагружению являются следующие акустические параметры образцов стали ХМ-12: скорость поперечной волны, коэффициент Пуассона, коэффициент двойного ЭМА-преобразования и коэффициент акустической анизотропии.

Ключевые слова: мартенситно-стареющая сталь ХМ-12; акустические свойства; термическая обработка; механическая растягивающая нагрузка; циклическое нагружение.

Благодарности: Исследование выполнено за счет гранта Российского научного фонда (грант № 22-19-00252, https://rscf.ru/project/22-19-00252/) с использованием УНУ «Информационно-измерительный комплекс для исследований акустических свойств материалов и изделий» (рег. номер 586308).

Статья подготовлена по материалам докладов участников XI Международной школы «Физическое материаловедение» (ШФМ-2023), Тольятти, 11–15 сентября 2023 года.

Для цитирования: Муравьева О.В., Муравьев В.В., Волкова Л.В., Владыкин А.Л., Белослудцев К.Ю. Акустические свойства мартенситно-стареющей стали ХМ-12 после энергетических воздействий // Frontier Materials & Technologies. 2024. № 2. С. 87–100. DOI: 10.18323/2782-4039-2024-2-68-8.